Calcitonin Forms Oligomeric Pore-Like Structures in Lipid Membranes

Marco Diociaiuti,* Laura Zanetti Polzi,* Luisa Valvo,† Fiorella Malchiodi-Albedi,‡ Cecilia Bombelli,§ and Maria Cristina Gaudiano†

*Dipartimento di Tecnologie e Salute, †Dipartimento del Farmaco, and ‡Dipartimento di Biologia Cellulare e Neuroscienze, Istituto Superiore di Sanità, 299-00161 Rome, Italy; and §CNR Istituto di Metodologie Chimiche and Dipartimento di Chimica, Università degli Studi di Roma "La Sapienza", 5-00185 Rome, Italy

ABSTRACT Calcitonin is a polypeptidic hormone involved in calcium metabolism in the bone. It belongs to the amyloid protein family, which is characterized by the common propensity to aggregate acquiring a β-sheet conformation and include proteins associated with important neurodegenerative diseases. Here we show for the first time, to our knowledge, by transmission electron microscopy (TEM) that salmon-calcitonin (sCT) forms annular oligomers similar to those observed for β-amyloid and α-sinuclein (Alzheimer's and Parkinson's diseases). We also investigated the interaction between sCT and model membranes, such as liposomes, with particular attention to the effect induced by lipid "rafts" made of cholesterol and G_{M1}. We observed, by TEM immunogold labeling of sCT, that protein binding is favored by the presence of rafts. In addition, we found by TEM that sCT oligomers inserted in the membrane have the characteristic pore-like morphology of the amyloid proteins. Circular dichroism experiments revealed an increase in β-content in sCT secondary structure when the protein was reconstituted in rafts mimicking liposomes. Finally, we showed, by spectrofluorimetry experiments, that the presence of sCT allowed Ca^{2+} entry in rafts mimicking liposomes loaded with the Ca^{2+}-specific fluorophore Fluo-4. This demonstrates that sCT oligomers have ion-channel activity. Our results are in good agreement with recent electrophysiological studies reporting that sCT forms Ca^{2+}-permeable ion channels in planar model membranes. It has been proposed that, beyond the well-known interaction of the monomer with the specific receptor, the formation of Ca^{2+} channels due to sCT oligomers could represent an extra source of Ca^{2+} entry in osteoblasts. Structural and functional data reported here support this hypothesis.

INTRODUCTION

Calcitonin (CT) is a 32-amino acid peptide involved in bone calcium metabolism and clinically used in the treatment of osteoporosis and other metabolic bone diseases. Its ability to lower the plasma calcium concentration has been widely studied and principally attributed to a strong inhibitory action on osteoclast-mediated bone resorption (1). It has been demonstrated that CT acts via a specific receptor found in many cell types and tissues, suggesting diverse biological roles for CT (2). In a recent work, Burns et al. demonstrated that CT gene-related peptide (CGRP) elevates calcium and polarizes membrane potential in MG-63 cells, an osteoblast cell line (3). They suggested that the peptide stimulates Ca^{2+} influx in part through L-type voltage-dependent channels.

In the study of CT physiological activity, its ability of forming aggregates has seldom been considered. However, CT is generally considered an amyloid protein due to its aggregation behavior, which starts with the formation of oligomers and eventually results in the deposition of fibrils and plaques. Some authors consider annular aggregates as ''off-pathway'' intermediates in the process of fibrilization (4). Unexpected results were obtained when it was shown that CT is neurotoxic in vitro in the same manner and more so than other amyloid proteins involved in neurodegenerative pathologies (5,6). Many studies have been carried out to investigate the relationship between structural features and toxicity of amyloid proteins involved in diseases, such as β-amyloid (βA) in Alzheimer's disease (AD), α-Synuclein (αS) in Parkinson's disease (PD), prion in Creutzfeldt-Jacob's disease, inslet amyloid polypeptide in type II diabetes, and others (7). Noticeably, Bucciantini et al. proved that oligomers of proteins not associated with any disease are also neurotoxic, suggesting that a shared structural feature of the amyloid oligomers is at the basis of neurotoxicity (8). This result is in good agreement with the general hypothesis that protein misfolding, leading to the exposure of hydrophobic regions of proteins, renders them potentially toxic, independent of their primary sequences (9). Misfolded proteins should have the ability to aggregate and interact with lipid membranes inducing cell damage and malfunction, mainly mediated via the formation of ion channels (7). Interestingly, this kind of toxicity named ''hydrophobicity-based toxicity'' is similar to those described for antibacterial toxins and viral proteins. This hypothesis is strongly supported by the observation that a single antibody, specifically designed for βA, is able to recognize soluble oligomers of widely varying primary sequences of amyloid proteins (10).

In this framework, Lashuel et al. found a common structural feature for the A30P and A53T αS mutations associated with PD and βA_{ARC} (arctic mutation) associated with AD (11). These proteins were shown to form oligomers rich in β-sheet secondary structure, conformed as annular protofibrils with a diameter ranging 7–12 nm. Lin et al. (12) showed that βA forms ion channels in lipid bilayers and imaged them for the first time by atomic force microscopy, suggesting that

Submitted December 9, 2005, and accepted for publication May 2, 2006.

Address reprint requests to Marco Diociaiuti, Tel.: 06-49902981; Fax: 06-49387140; E-mail: marco.diociaiuti@iss.it.

0006-3495/06/09/2275/07 $2.00

doi: 10.1529/biophysj.105.079475

they were composed of hexamers or tetramers. Moreover, they measured the channel conductivity and tested the channel biological activity on neurons, demonstrating that βA pore formation induces rapid neuritic degeneration and death by a Ca^{2+}-dependent toxicity mechanism (12). The pore formation and channel-like activity have been recently described for other amyloid proteins, suggesting a possible common mechanism for protein-misfolding diseases (13). A Ca^{2+}-dependent toxicity, based on pore-like protofibrils that cause membrane permeabilization, has been proposed for αS by Volles et al. in PD (14,15).

Theoretical models have been proposed to predict βA peptide ability to insert in lipid bilayer (16). Molecular dynamic simulation has been developed for βA ion-channel formation in lipid bilayer on the basis of the amino acid sequence and experimental evidence of multilevel ion-channel conductance. Several pore arrangements can be obtained, all starting from a basic structure composed of a β-hairpin followed by a helix-turn-helix motif (17).

Finally, it has been widely demonstrated that the secondary structure of membrane-bound βA and its ability to insert into the lipid membrane are strongly affected by the lipid composition. In particular, the importance of ''raft-like'' lipid domains in the membrane has been recently pointed out, with particular attention to the presence of gangliosides (18). In particular, Kakio et al. showed that low ganglioside content favors the β-structure conformation (19,20).

Here we report for the first time, to our knowledge, transmission electron microscopy (TEM) evidence of salmon calcitonin (sCT) annular oligomers very similar to those described for other amyloid proteins. Moreover, sCT oligomers form Ca^{2+}-permeable pores when inserted into rafts containing liposomes. Circular dichroism (CD) data demonstrate that the protein β-structure content increases during the interaction with lipids.

MATERIALS AND METHODS

Preparation of sCT and sCT-liposome solutions

Lyophilized sCT (molecular mass = 3432 Da) was purchased from European Pharmacopoeia (EDQM, Strasbourg, France) and stored at −18°C before use. L-α-phosphatidylcholinedipalmitoyl 99% (molecular mass = 734 Da), cholesterol 99+% (molecular mass = 387 Da), and monosialoganglioside-G_{M1} 95% from bovine brain (molecular mass = 1564 Da) were purchased from Sigma (Sigma Chemical, St Louis, MO) and stored at −18°C before use. Fluo-4 was purchased from Molecular Probes (Eugene, OR) and stored at −18°C before use. All reagents were of analytical grade. sCT 0.04 mg/ml solution (corresponding to 1.2×10^{-5} M protein content) was prepared by dissolving the protein in the solid state in 5 mM sodium phosphate buffer, pH 7.4—a condition that facilitates oligomerization (21). To avoid the formation of fibrils, the solutions were prepared immediately before use. For the same reason, no stock solutions of protein were employed. For liposome preparation, two different lipid solutions were prepared in chloroform: i) dipalmitoylphosphatidylcholine (DPPC), and ii) DPPC/cholesterol/G_{M1} (50:46:4 mol %) by dissolving 3.7 mg of total lipids in ~12 ml chloroform. sCT-containing liposomes were prepared by adding to both lipid chloroform solutions 1.0 mg of sCT dissolved in 3 ml of methanol. The obtained mixtures were placed in 100-ml round-bottomed flasks connected with a rotary evaporation unit, and the solvent was evaporated to form sCT-lipid films. The films were dried by a vacuum pump overnight. After drying, for CD and TEM analyses the films were rehydrated by 2.5 ml of phosphate buffer (5 mM, pH 7.4) for Ca^{2+} influx measurements by 2.5 ml of HEPES/EGTA buffer (5 mM/0.1 mM, pH 7.4) added with Fluo-4 (20 μM). The solutions were vortex mixed and then freeze thawed six times from liquid nitrogen to 325 K. Dispersions were then extruded (10 times) through a 100-nm polycarbonate membrane (Whatman Nucleopore, Clifton, NJ). The extrusions were carried out at 325 K, well above the transition temperature of DPPC (315 K), using a 2.5-ml extruder (Lipex Biomembranes, Vancouver, Canada). The solutions were then diluted 1:10 with buffer for CD and TEM analyses to obtain the same protein concentration of the ''in buffer'' experiments.

Transmission electron microscopy

Negative stain was obtained by a phosphotungstic acid (PTA) 2% w/v solution buffered at pH = 7.3 with NaOH. To avoid salt precipitation from PTA and/or NaOH, which can be misinterpreted as actual structures, the staining solution was filtered before each preparation through polycarbonate 0.2-μm pore filters. A droplet of the suspension, containing liposomes and proteins, was deposited onto 300 mesh copper grids for electron microscopy and covered with a very thin amorphous carbon film (~20 nm), and the excess of liquid was removed by placing the grid on filter work. When the grid was dried, a droplet of the staining solution was deposited and dried following the same procedure. The heavy metal (W) surrounding the specimen to be imaged scatters electrons more efficiently than the specimen itself, providing high image contrast and allowing a detailed examination of the structure (22). Moreover, heavy metal salts give good radiation protection and maintain the structural integrity under the electron beam bombardment. The samples were studied in a Zeiss 902 transmission electron microscope (Zeiss, Jena, Germany) operating at 80 kV and equipped with an electron energy loss filter. To enhance the contrast, the microscope was used in the electron spectroscopy imaging (ESI) mode filtering at $\Delta E = 0$ eV. The image acquisition was performed by a digital charge-coupled device camera model HSC2, 1k for 1k pixels, (Proscan, Lagerlechfeld, Germany), thermostated by a Peltier cooler model WKL 230 (LAUDA, Lauda-Königshofen, Germany). Image analysis and quantification was performed by a digital image analyzer analySIS 3.0 (SiS, Klausdorf, Germany). This software allows us to enhance contrast and sharpness of the acquired images and to perform morphological quantification and statistics. The dimensional measurements were performed after a careful magnification calibration of the whole imaging system based on reference standards (cross grating and catalase crystal). For statistical analysis, ~260 objects were considered from at least five fields.

sCT immunogold labeling

sCT liposomes were deposited onto thin carbon film-coated grids for TEM observation and air dried. For immunolocalization of sCT, samples were preincubated for 5 min with 1% w/v bovine serum albumin (BSA) (Sigma Chemical, St. Louis, MO) in phosphate buffer (0.1 M, pH 7.0) and then incubated for 30 min at room temperature with mouse monoclonal anti-sCT (Abcam, Cambridge, UK) at a concentration of 40 μg/ml. After washing for 10 min by floating the grids on phosphate buffer drops containing 1% w/v BSA, samples were labeled with anti-mouse IgG 5-nm gold conjugate diluted 1:10 (Sigma Chemical) for 30 min at room temperature. Control samples were obtained as described above both by omission of the primary antibody and on liposomes without sCT. After washing with phosphate buffer, samples were negatively stained with PTA as described above.

Circular dichroism measurements

CD measurements were performed on a Jasco J-710 spectropolarimeter (Jasco, Tokyo, Japan) in the far-ultraviolet region (260–195 nm). All spectra

recorded were blank subtracted and were the mean of 8–16 different scans. Quartz cells of 0.1-cm path length were employed. The spectral step resolution was 0.1 nm and the speed scan 20 nm/min. All CD spectra were reported as $\Delta\varepsilon = [\Theta]/3300$, where $[\Theta]$ is equal to $(\theta \times 100)/(l \times C)$ (θ is the measured ellipticity, C is the aminoacid concentration ($= 1.2 \times 10^{-5} \times 32$), and l is the path length in centimeter). Conformational analyses of CD spectra were performed using the CDSSTR routine in a software package for analyzing protein CD spectra via the Internet (23).

Ca^{2+} influx measurements

Ca^{2+} influx was measured using Fluo-4 as Ca^{2+} indicator dye. Fluo-4 non-entrapped in liposomes was separated by filtration of 200 μl of liposomes solution on a 1-ml Biorad (Hercules, CA) AM-15 gel column, equilibrated in HEPES/EGTA buffer solution. Fractions containing liposomes were identified, with the first five fractions that were combined and diluted to 2 ml. Fluorescence measurements were performed at room temperature with a Shimadzu (Columbia, MD) RF5001PC spectrofluorimeter in a 1-cm cuvette. Excitation wavelength was 494 nm, whereas emission intensity was revealed in the range 500–540 nm with slits set to 5 mm. Ca^{2+} influx was induced by addition of 20 μl of 17.2 mM $CaCl_2$ to the cuvette to obtain a final calcium concentration (0.172 mM) that does not cause fusion of liposomes and dispersion of the dye in the bulk (24).

RESULTS AND DISCUSSION

In previous articles, we investigated the early stages of sCT aggregation induced by ageing or oxidative conditions (25,26). In this work we report, for the first time, to our knowledge, images of annular sCT oligomers of shape and dimension very similar to βA and αS protofibrils described in the literature.

Fig. 1 shows negatively stained sCT annular oligomers observed by TEM. The statistical distribution of their circle perimeters is also shown. As reported for βA, also in the case of sCT, the dominant symmetry was hexagonal even if small globules and incomplete hexagons and/or linear protofibrils were also observed. Considering sCT low molecular weight, the small globules could be oligomers themselves and the annular structures could be assemblies of oligomers. This structural feature has been described for βA and αS and is considered to be at the basis of the ''hydrophobicity-based neurotoxicity''. However, sCT is not directly involved in any neurologic disease, even if, unexpectedly, its neurotoxicity was observed in in vitro experiments (5,6).

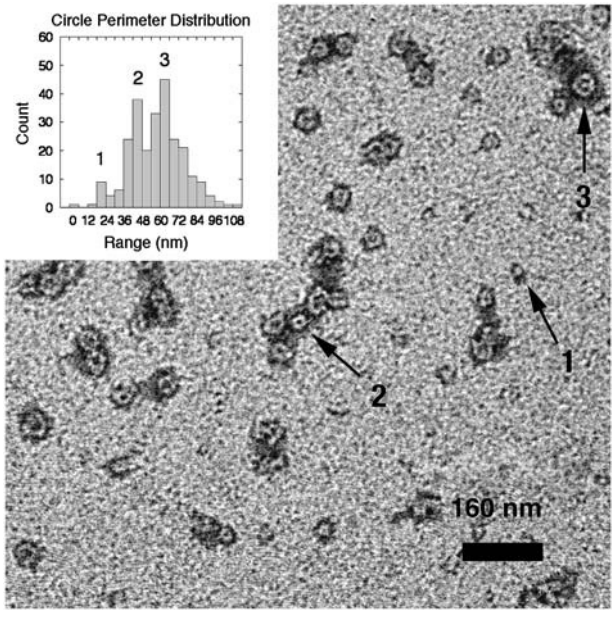

FIGURE 1 sCT annular oligomers imaged by negative contrast TEM. The inset shows the oligomer dimensional distribution (~260 objects). The arrows indicate typical particles corresponding to each class.

We reconstituted sCT in DPPC liposomes and in rafts containing liposomes (DPPC/cholesterol/monoganglioside-G_{M1}) to investigate the differences in the interaction of the protein with these two model membranes, with particular attention to the effect induced by the presence of lipid rafts (27).

Immunogold labeling (Fig. 2) performed on sCT reconstituted in DPPC/cholesterol/G_{M1} liposomes allowed us to demonstrate that the protein strongly binds to rafts containing liposomes, whereas plain DPPC liposomes were seldom decorated, as we previously reported (26). This experiment clearly indicates that a specific stronger interaction of sCT with rafts occurred.

Fig. 3 shows TEM images of rafts containing liposomes opened onto amorphous carbon substrate in the presence of sCT. Gray islands surrounded by a dark background characterize the images. They represent liposomes opened and fused with each other, together with some unopened liposomes that appear white (28). As can be observed in Fig. 3, annular structures are easily recognizable on the dark background. Fig. 3, *B* and *C*, shows high magnification images of two different annular oligomers not interacting with

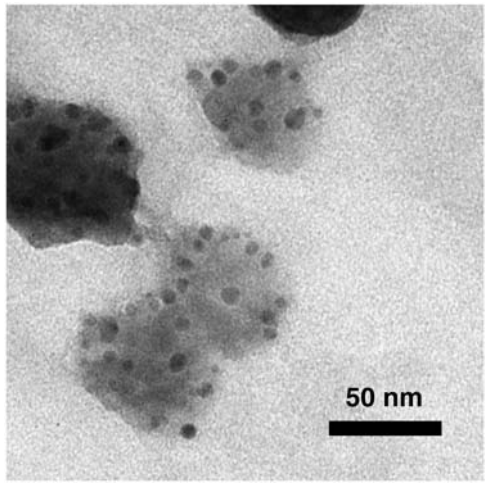

FIGURE 2 sCT strongly binds to liposomes made of DPPC/cholesterol/G_{M1} mimicking the occurrence of lipid rafts in the lipid membranes. Immunogold labeling TEM, performed with anti-mouse IgG 5-nm gold conjugate, clearly reveals that sCT is localized at the liposome surface. Conversely, only a few gold particles have been found around liposomes made of plain DPPC (26).

liposomes, very similar in shape and dimension to those reported in Fig. 1 in the absence of liposomes. More interestingly, annular structures are also often detectable in liposomes, as shown in Fig. 3, *D* and *E*. They seem to be smaller than the isolated ones and characterized by a hexagonal symmetry. The diameter of the internal pores of these structures was ~3 nm. This is compatible with the pore size of most Ca^{2+}-permeable channels. In our opinion, they represent the direct visualization of the ion channels formed by sCT in the lipid bilayer. It is worth noting that these annular structures were never observed in the samples of both sCT- and raft-free liposomes.

These findings strongly suggest that sCT annular oligomers interact with the lipid bilayer-containing rafts, likely forming Ca^{2+}-permeable channels, as previously proposed by Stipani et al. (29) on the basis of electrophysiological measurements. This is the first direct evidence, to our knowledge, of sCT channel formation in a lipid environment and is in good agreement with the observation of pores formed by many other amyloid proteins reconstituted in liposomes and studied by atomic force microscopy (13). Moreover, the hexagonal symmetry has been proposed in the numerical simulation of the amyloid channels (17).

Fig. 4 shows CD spectra of sCT in the presence of liposomes, with or without rafts, together with the relative percentages of α-, β-, and unordered structures obtained by deconvolution software (23). It is well known that the aggregation process of amyloid proteins is generally accompanied by an increase in β-content (26,30). An evident rising of the β-structure and a corresponding reduction of the random-coil content can be observed in rafts containing samples, whereas an essentially random-coil structure, very similar to the typical sCT conformation in water (26), is observed in plain DPPC liposomes. This conformational change can be clearly attributed to the interaction of sCT

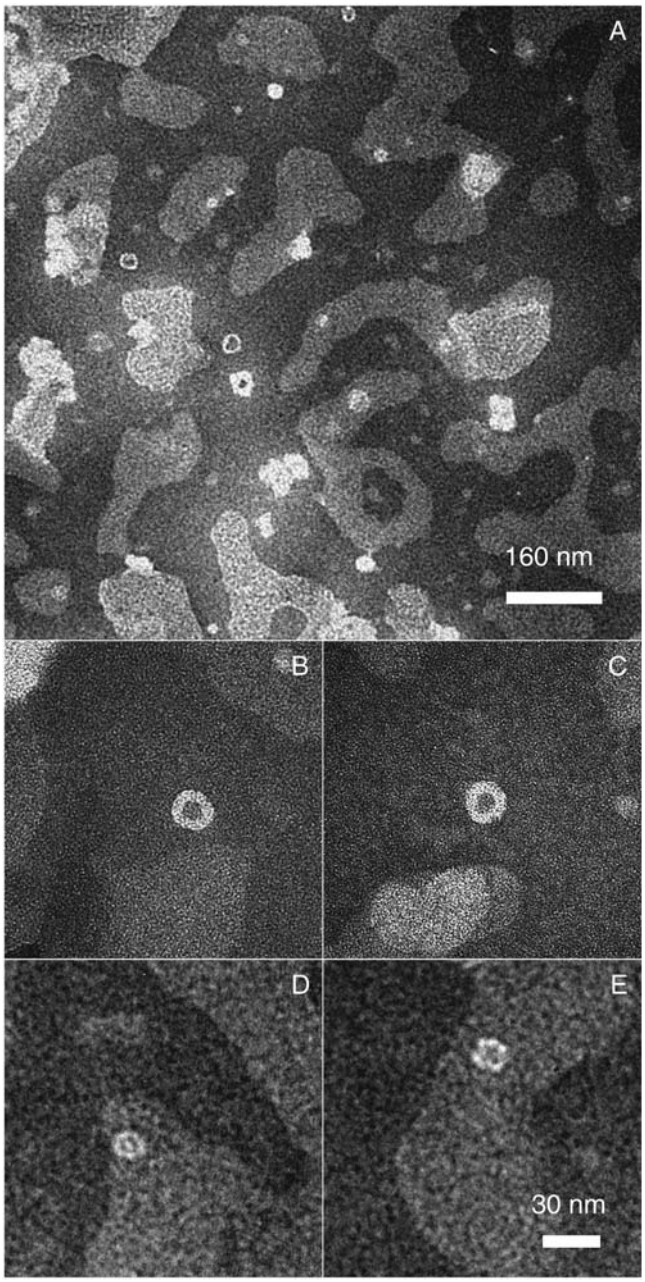

FIGURE 3 Rafts containing liposomes (*gray islands*) opened on amorphous carbon substrate for TEM in the presence of sCT (*A*). Isolated annular structures, similar to those observed in Fig. 1, are clearly detectable as ''doughnuts'' in the dark background (high magnification in *B* and *C*). More interestingly, pore-like structures are clearly observable in liposomes (high magnification in *D* and *E*). Such features are quite repetitive and characterized by a hexagonal symmetry.

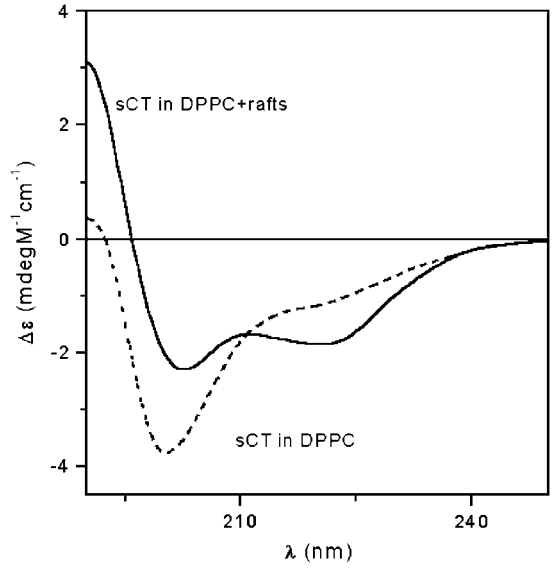

FIGURE 4 CD spectra of sCT reconstituted in two different types of liposomes: plain DPPC (*dashed line*) and DPPC/cholesterol/G_{M1} (*continuous line*). Liposomes containing cholesterol/G_{M1} mimic the occurrence of lipid rafts. The deconvolution of the CD curves gives (Random = 56%; Turn = 15%; α-helix = 5%; β-structures = 23%) in the absence and (Random = 46%; Turn = 19%; α-helix = 5%; β-structures = 30%) in the presence of rafts. As can be observed the random-coil content decreases, whereas β content rises in the presence of rafts.

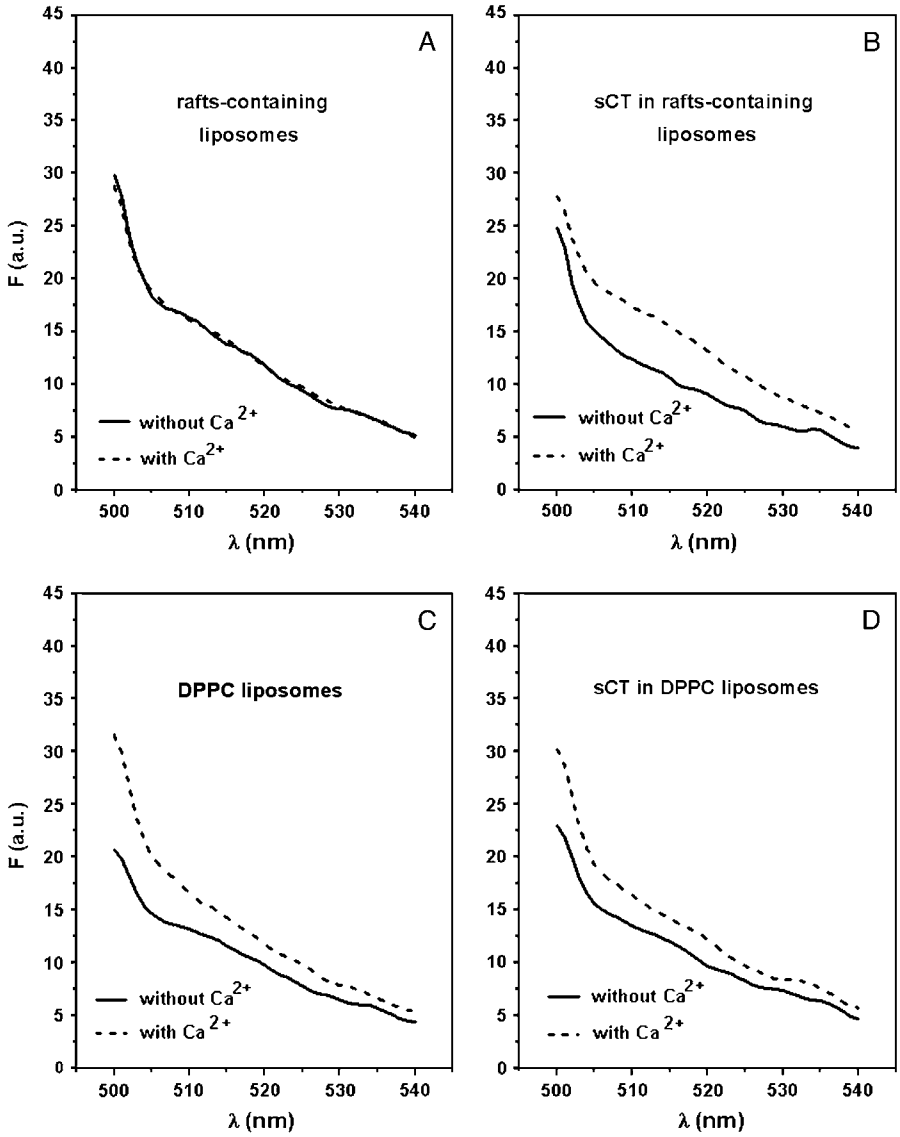

FIGURE 5 Fluorescence spectra relative to Ca^{2+} influx experiments performed on liposomes loaded with Fluo-4. Liposomes made of DPPC/cholesterol/G_{M1}, mimicking the occurrence of lipid rafts (*A*, *B*), give a fluorescence signal after the addition of Ca^{2+} only when sCT is inserted in the membrane (*B*). Plain DPPC liposomes (*C*, *D*) do not change the fluorescence signal in the presence of sCT, demonstrating that Ca^{2+} enters liposomes only when both sCT and rafts are present.

with the lipid rafts. Our result is very similar to that published for ganglioside-bound βA (19) and is consistent with the secondary structure foreseen in the theoretical models (molecular dynamic) of ion channels (17).

Finally, Fig. 5 shows fluorescence spectra of liposomes loaded by Fluo-4. The presence of sCT reconstituted in rafts containing liposomes allows Ca^{2+} entry, whereas the addition of Ca^{2+} in the solution of plain rafts containing liposomes does not alter the spectral shape. This result demonstrates that Ca^{2+} enter liposomes only when sCT is present and strongly suggests that the pore-like structures observed in the lipid bilayer are Ca^{2+}-permeable ion channels.

In addition, we found that the presence of rafts is required for Ca^{2+} entry, since fluorescence spectra of plain DPPC liposomes do not evidence any significant difference after the reconstitution of sCT (Fig. 5, *C* and *D*). This result supports the strategic role played by lipid rafts in facilitating the membrane insertion of amyloid proteins.

All our results showed a dramatic similarity between βA, αS, and sCT oligomers. In particular, we observed an annular morphology for sCT similar to the one observed for the A30P and A53T αS and βA_{ARC} mutations (11), and we directly visualized that these structures actually interact with lipids. Moreover, in agreement with CD data relative to other amyloids (11,19), we found an increase in β secondary structure when sCT interacts with model membranes containing rafts. Finally, we show that annular oligomers are permeable to Ca^{2+}, providing a demonstration of their functional activity as in the case of βA. This activity is strictly dependent on the presence of rafts, substantiating their role in the possibly harmful pore formation.

All these structural and functional data are in good agreement with the general hypothesis (9) that protein

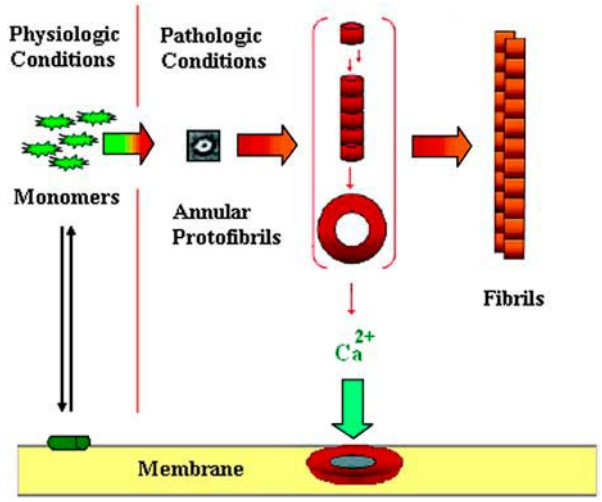

FIGURE 6 Schematic representation of the model proposed by Volles et al. (15) to explain how αS induces calcium-dependent neurotoxicity in PD. Annular oligomers organize in a structure that interacts with the lipid bilayer forming harmful Ca^{2+}-permeable channels.

misfolding leads to the exposure of hydrophobic regions and renders proteins potentially cytotoxic via the formation of ion channels. In addition, these results again corroborate the hypothesis that amyloid proteins, although lacking sequence homology, have a similar aggregation behavior. It is interesting to note that CT has been found to be toxic for neurons in vitro (5,6).

Most CT activities are mediated by a G protein-coupled transmembrane receptor in osteoclasts (2). Recently, it has been proposed that CT could form ion channels in osteoblast plasma membrane, leading to Ca^{2+} influx (29). Here we provide, for the first time, experimental evidence that sCT oligomerization actually leads to the formation of annular structures able to interact with model membranes, in the presence of lipid rafts, with Ca^{2+}-permeable channel activity.

CONCLUSIONS

The structural investigation here reported clearly indicates that sCT, physiologically involved in the regulation of calcium in the bone tissue, is able to form annular oligomers during the early stages of fibrillar aggregation. These oligomers are very similar to those observed for proteins involved in important neurodegenerative diseases, such as AD and PD. Moreover, the presence of rafts in model membranes strongly favors the binding of sCT, with the consequent increase of its β-secondary structure content. Conversely, sCT interacts slightly with plain DPPC liposomes, without any significant conformational modification (26). The annular sCT oligomers have been directly visualized in the interaction with raft-containing liposomes, forming amyloid ion channels. Finally, we demonstrate that these structures play a functional role, allowing Ca^{2+} to cross the lipid membranes. It is worth noting that in the absence of rafts, sCT reconstituted in plain DPPC liposomes does not induce Ca^{2+} entry.

Recently, a mechanism has been proposed (schematically represented in Fig. 6) based on the formation of pore-like oligomers that penetrate the lipid bilayer to explain the neurotoxicity of several amyloid proteins (15). However, we wonder if this mechanism also has physiological significance in the case of the role played by CT in calcium homeostasis.

We thank Dr. Giovanna Mancini of the National Research Council, Istituto di Metodologie Chimiche, and Dipartimento di Chimica, Università degli Studi di Roma ''La Sapienza'' for the kind cooperation and helpful discussions, and Mr. Carmine De Sena of Dipartimento del Farmaco, Istituto Superiore di Sanità, for technical assistance.

This research was supported by a grant from the Italian National Health Fund for the project ''Safety of Drugs Used in Diseases of the Elderly'' (Progetto 1%—Ricerca Sanitaria Finalizzata 2000).

REFERENCES

1. Wallach, S., G. Rousseau, L. Martin, and M. Azria. 1999. Effects of calcitonin on animal and in vitro models of skeletal metabolism. *Bone*. 25:509–516.
2. Findlay, D. M., and P. M. Sexton. 2004. Calcitonin. *Growth Factors*. 22:217–224.
3. Burns, D. M., L. Stehno-Bittel, and T. Kawase. 2004. Calcitonin gene-related peptide elevates calcium and polarizes membrane potential in MG-63 cells by both camp-independent and -dependent mechanisms. *Am. J. Physiol. Cell Physiol.* 287:C457–C467.
4. Wacker, J. L., M. H. Zareie, H. Fong, M. Sarikaya, and P. J. Muchowski. 2004. Hsp70 and Hsp40 attenuate formation of spherical and annular polyglutamine oligomers by partitioning monomer. *Nat. Struct. Mol. Biol.* 11:1215–1222.
5. Schubert, D., C. Behl, R. Lesley, A. Brack, R. Dargusch, Y. Sagara, and H. Kimura. 1995. Amyloid peptides are toxic via a common oxidative mechanism. *Proc. Natl. Acad. Sci. USA*. 92:1989–1993.
6. Wang, S. S., T. A. Good, and D. L. Rymer. 2005. The influence of phospholipid membranes on bovine calcitonin peptide's secondary structure and induced neurotoxic effects. *Int. J. Biochem. Cell. Biol.* 37:1656–1669.
7. Kagan, B. L., R. Azimov, and R. Azimova. 2004. Amyloid peptide channels. *J. Membr. Biol.* 202:1–10.
8. Bucciantini, M., E. Giannoni, F. Chiti, F. Baroni, L. Formigli, J. Zurdo, N. Taddei, G. Ramponi, C. M. Dobson, and M. Stefani. 2002. Inherent toxicity of aggregates implies a common mechanism for protein misfolding diseases. *Nature*. 416:507–511.
9. Kourie, J. I., and C. L. Henry. 2002. Ion channel formation and membrane-linked pathologies of misfolded hydrophobic proteins: the role of dangerous unchaperoned molecules. *Clin. Exp. Pharmacol. Physiol.* 29:741–753.
10. Kayed, R., E. Head, J. L. Thompson, T. M. McIntire, S. C. Milton, C. W. Cotman, and C. G. Glabe. 2003. Common structure of soluble amyloid oligomers implies common mechanism of pathogenesis. *Science*. 300:486–489.
11. Lashuel, H. A., D. Hartley, B. M. Petre, T. Walz, and P. T. J. Lansbury. 2002. Amyloid pores from pathogenic mutations. *Nature*. 418:291.
12. Lin, H., R. Bathia, and R. Lal. 2001. Amyloid β protein forms ion channel: implications for Alzheimer's disease pathophysiology. *FASEB J.* 15:2433–2444.
13. Quist, A., I. Doudevski, H. Lin, R. Azimova, D. Ng, B. Frangione, B. Kagan, J. Ghiso, and R. Lal. 2005. Amyloid ion channels: a common structural link for protein-misfolding disease. *Proc. Natl. Acad. Sci. USA*. 102:10427–10432.

14. Volles, M. J., and P. T. J. Lansbury. 2002. Vesicle permeabilization by protofibrillar α-synuclein is sensitive to Parkinson's disease-linked mutations and occurs by a pore-like mechanism. *Biochemistry.* 41:4595–4602.

15. Volles, M. J., and P. T. J. Lansbury. 2003. Zeroing in on the pathogenic form of α-synuclein and its mechanism of neurotoxicity in Parkinson's disease. *Biochemistry.* 42:7871–7878.

16. Mobley, D. L., D. L. Cox, R. R. Singh, M. W. Maddox, and M. L. Longo. 2004. Modeling amyloid beta-peptide insertion into lipid bilayers. *Biophys. J.* 86:3585–3597.

17. Durell, S. R., H. R. Guy, N. Arispe, E. Rojas, and H. B. Pollard. 1994. Theoretical models of the ion channel structure of amyloid β-protein. *Biophys. J.* 67:2137–2145.

18. Simons, K., and D. Toomre. 2000. Lipid rafts and signal transduction. *Nat. Rev. Mol. Cell Biol.* 1:31–39.

19. Kakio, A., S. Nishimoto, K. Yanagisawa, Y. Kozutsumi, and K. Matsuzaki. 2001. Cholesterol-dependent formation of GM1 ganglioside-bound amyloid β-protein, an endogenous seed for Alzheimer amyloid. *J. Biol. Chem.* 276:24985–24990.

20. Kakio, A., S. Nishimoto, K. Yanagisawa, Y. Kozutsumi, and K. Matsuzaki. 2002. Interactions of amyloid β-protein with various gangliosides in raft-like membranes: importance of GM1 ganglioside-bound form as an endogenous seed for Alzheimer amyloid. *Biochemistry.* 41:7385–7390.

21. Stine, W. B. Jr., K. N. Dahlgren, G. A. Krafft, and M. J. LaDu. 2003. In vitro characterization of conditions for amyloid-beta peptide oligomerization and fibrillogenesis. *J. Biol. Chem.* 278:11612–11622.

22. Diociaiuti, M. 2005. Electron energy loss spectroscopy microanalysis and imaging in the transmission electron microscope: example of biological applications. *J. Electron. Spectrosc.* 143:189–203.

23. Whitmore, L., and B. A. Wallace. 2004. DICHROWEB, an online server for protein secondary structure analyses from circular dichroism spectroscopic data. *Nucleic Acids Res.* 32:668–673.

24. Fraley, R., J. Wilschut, N. Duzgunes, C. Smith, and D. Papahadjopoulos. 1980. Studies on the mechanism of membrane fusion: role of phosphate in promoting calcium ion induced fusion of phospholipid vesicles. *Biochemistry.* 19:6021–6029.

25. Gaudiano, M. C., M. Diociaiuti, P. Bertocchi, and L. Valvo. 2003. Effects induced by hydroxyl radicals on salmon calcitonin: an RP-HPLC, CD and TEM study. *Biochim. Biophys. Acta.* 1623:33–40.

26. Gaudiano, M. C., M. Colone, C. Bombelli, P. Chistolini, L. Valvo, and M. Diociaiuti. 2005. Early stages of salmon calcitonin aggregation: effects induced by ageing and oxidation processes in water and in the presence of model membranes. *Biochim. Biophys. Acta.* 1750:134–145.

27. Yuan, C., and L. J. Johnston. 2000. Distribution of ganglioside GM1 in L-α-dipalmitoylphospatidylcholine/cholesterol monolayers: a model for lipid rafts. *Biophys. J.* 79:2768–2781.

28. Diociaiuti, M., A. Molinari, I. Ruspantini, M. C. Gaudiano, R. Ippoliti, E. Lendaro, F. Bordi, P. Chistolini, and G. Arancia. 2002. P-glycoprotein inserted in planar lipid bilayer formed by liposomes opened on amorphous carbon and Langmuir-Blodgett monolayer. *Biochim. Biophys. Acta.* 1559:21–31.

29. Stipani, V., E. Gallucci, S. Micelli, V. Picciarelli, and R. Benz. 2001. Channel formation by salmon and human calcitonin in black lipid membranes. *Biophys. J.* 81:3332–3338.

30. Apetri, M. M., N. C. Maiti, M. G. Zagorski, P. R. Carey, and V. E. Anderson. 2006. Secondary structure of alpha-synuclein oligomers: characterization by Raman and atomic force microscopy. *J. Mol. Biol.* 355:63–71.